Onset criterion for a turbulence-driven ionization instability in hollow cathodes

IEPC-2019-155

Presented at the 36th International Electric Propulsion Conference
University of Vienna, Austria
September 15–20, 2019

Marcel P. Georgin,* Benjamin A. Jorns,† and Alec D. Gallimore‡
University of Michigan, Ann Arbor, MI 48109

An analytical stability criterion is derived for a wave-driven ionization instability under the assumption that the growth of ion acoustic turbulence is the destablizing factor for this low-frequency mode. This criterion, along with the underlying assumptions of the theory, are investigated experimentally and shown to be met during plume mode operation of the cathode. The predicted real frequency is on the same order as the experimentally observed oscillation. Time-dependent plasma properties are investigated and are shown to be in qualitative agreement with theoretical expectations. The analytical onset criterion is recast into cathode operating parameters and shown to agree with previously determined empirical scaling laws.

*Ph.D Candidate, Applied Physics Program, georginm@umich.edu

†Assistant Professor, Department of Aerospace Engineering

‡Robert J. Vlasic Dean of Engineering, the Richard F. and Eleanor A. Towner Professor of Engineering, and Arthur F. Thurnau Professor of Aerospace Engineering

Nomenclature

A_o	= Cathode orifice area
c_s	= Ion sound speed
E	= Electric field
I_{sat}	= Ion saturation current
I_{dc}	= Discharge current
k	= Wave vector
m_e	= Electron mass
m_i	= Ion mass
$\dot{m}$	= Mass flow rate
n	= Plasma density
p_k	= Wave momentum
q	= Unit charge
T_e	= Electron temperature
T_i	= Ion temperature
u_e	= Electron drift velocity
u_i	= Ion drift velocity
v_e	= Electron thermal velocity
V_f	= Floating potential
Φ	= Plasma potential
ν	= Total collision frequency
ν_{an}	= Anomalous collision frequency
ν_{ion}	= Ionization frequency
γ_{IAT}	= Turbulence growth rate
γ_{ion}	= Response rate of ionization to temperature
ω_r	= Real frequency of oscillation
ω_i	= Imaginary frequency of oscillation

I. Introduction

The effects of plasma turbulence is an intense area of research for the electric propulsion (EP) community as it is a critical driver of the plasma state in many EP devices. To name some examples, turbulence is known to drive the resistivity in the plume of hollow cathodes and is thought to play an important role in cross-field transport in Hall thrusters. Gaps in our understanding of these collective effects of turbulence can prevent the self-consistent modeling of EP devices. Ultimately, without high-fidelity codes that can account for these effects, design and flight qualification through modeling alone remains impossible and predicting long-term behavior of EP systems is difficult.

Historically, the hollow cathodes found in Hall and ion thrusters have been challenging to model numerically.[1] Some notable examples are predicting the resistivity of the cathode plume[1,2] and the spot-to-plume mode transition.[3–6] As was posited by others, the plasma conditions produced by the cathode are ripe for the excitation of electrostatic turbulence, notably ion acoustic turbulence (IAT) that can raise the apparent resistivity of the plume.[7–9] Subsequent experimental measurements[10?,11] have shown that this turbulence utterly dominates the steady-state properties of the plasma. Without including its effects, notably the enhanced electron resistivity, it is not possible to accurately predict key plasma parameters, such as the plasma potential in the cathode plume[2,12,13].

Another pressing challenge in our understanding of hollow cathode physics is the origins of the so-called spot-to-plume mode transition. The spot mode has been shown to be dominated by the aforementioned small-scale electrostatic turbulence, whereas the plume mode exhibits large-scale, low frequency potential and density fluctuations that are thought to be the result of an ionization instability.[14] In extreme cases, these waves have been shown to drastically increase the ion energy and results in an order of magnitude greater erosion of cathode surfaces. Experimentally, this mode transition (the change in dominance from the IAT to the ionization instability) can be induced by reducing the gas flow rate to the device for a given geometry and current; however, to date there is no analytically derived onset criterion or intuitive physical interpretation for this ionization instability associated with the cathode plume mode.

Initial clues for how to describe this instability came from experimental measurements and high-fidelity numerical models that have linked the plasma oscillation with ionization and the presence of the underlying IAT. Seminal measurements by Goebel et al.[14] showed that amplitude and frequency of oscillation were consistent with an ionization-type wave. Later, it was showed in Ref. 15 that fluctuations in the IAT amplitude are highly correlated with oscillations in density and the total plasma resistivity.[16] From the modeling side, Refs. 17 and 18 both recovered coherent oscillations that qualitatively resemble these experimental measurements exclusively when the effects of IAT were included in their numerical models. These authors proposed that the instability may be caused by wave-driven heating due to the resistive effects of the IAT on electrons leading to an ionization wave. It is interesting to note that these numerical simulations use different closure models for the IAT. Ref. 17 assumes that the IAT has saturated while Ref. 18 have allowed for the wave energy to grow and convect. This is to say that there has yet to be a consensus on how to appropriately model the turbulence. From a theoretical perspective, the idea that wave-driven heating of electrons onsets an ionization instability is compelling; however there is no clear physical reasoning behind why this should result in the growth of an unstable mode.

Given the deleterious effects of this instability on cathode performance and the lack of physical understanding of its origins, there is an apparent need for an improved fundamental understanding of the mechanism that drives the plasma unstable and its relationship to the presence of IAT. Moreover, the predictive capability of the model must be assessed through experiment. To this end, we have organized this article in the following manner. First we provide a brief overview of the effects of IAT on the fluid plasma parameters and then derive a model for the onset of the ionization wave based on the growth of the IAT. In this section, we also examine the various closure models used in numerical models and how they compare with our onset-criterion. Then we describe the experimental techniques we used to measure plasma properties to evaluate the theory. Lastly, we conclude with some remarks about how our results may be used to guide cathode design.

II. Overview of IAT Theory

Although the growth of the IAT is a result of a kinetic resonance between the drifting electrons and ion sound waves, its growth and effects can be thought of in a fluid framework. The IAT can onset when the electron drift velocity exceeds the ion sound speed; however, the waves can be damped by collisional processes or kinetic effects such as ion Landau damping. The growth rate of the IAT is given by[19]

$$\gamma_{IAT} = \sqrt{\frac{\pi}{2}} k c_s \left(\frac{u_e - (c_s + u_i)}{v_e} - \left(\frac{T_e}{T_i}\right)^{3/2} e^{-T_e/2T_i} \right) - \frac{1}{2}\nu_{in} \tag{1}$$

where k is the wavevector, c_s is the ion sound speed, and u_e and v_e are the electron drift and thermal velocities, respectively. The parameter, ν_{in}, is the ion-neutral collision frequency and T_e and T_i are the electron and ion temperatures, respectively. Since the waves grow at the expense of the electron drift velocity, these waves act as a drag force on the electrons, and can be thought of as raising the effective collision frequency between electron and ions. This so-called anomalous collision frequency is determined through a momentum balance of the electrons with the wave momentum and is given by

$$\nu_{an} = \frac{1}{n u_e m_e} \sum_k p_k \gamma_k v_g \tag{2}$$

where the sum is over the IAT modes of wavenumber k and $p_k = W_k/\omega(k)$ is the momentum density of each mode in the IAT spectrum, W_k is the wave energy density of each mode, and v_g is the group velocity. The momentum transfer rate for a given mode, $\gamma_k = k c_s \sqrt{\frac{\pi}{2}} \frac{u_e}{v_e}$, is equal to the the growth component of γ_{IAT}. Eqn. 2 tells us that a mode containing a greater energy density will more rapidly accrue momentum from the electron fluid. This wave energy density, is a conserved quantity that propagates in space and time and grows according to the wave kinetic equation.

$$\frac{\partial W_k}{\partial t} + \nabla \left(v_g W_k \right) = W_k \left(\gamma_{IAT} \right) \tag{3}$$

Applying the dispersion of the IAT, assuming the ion drift is small and the ions are cold, we can show that the wave energy of an IAT mode is

$$W_k = \left(\frac{\tilde{\Phi}_k}{T_e} \right)^2 n T_e \ . \tag{4}$$

where $\tilde{\Phi}_k$ is the potential fluctuations of an IAT mode. Eqn. 4 tells us that larger plasma potential fluctuations lead to an increased wave energy whereas higher electron temperatures reduce it. Because the anomalous collision frequency depends on the wave energy density, fluctuations in W_k can ultimately lead to variations in Ohmic heating of the electrons. It is this heating that is thought to play a crucial role in the development of the ionization instability associated with plume mode.

III. Theory for Turbulence-driven Ionization Instability

In this section we present a zero-dimensional theory for the ionization instability present in hollow cathode plumes. But before addressing the details of the theory, first we discuss the physical

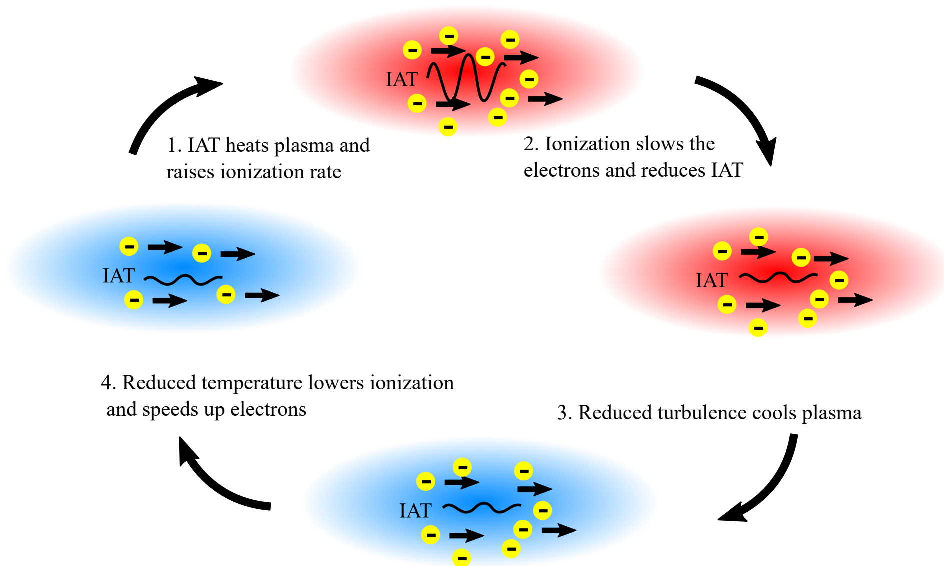

Fig. 1 Physical picture for plasma instability

mechanism behind the instability. Figure 1 shows, conceptually, the mechanism we propose for how turbulence can drive this ionization oscillation. Suppose the cathode discharge begins in a state where the plasma is cold, electrons are streaming and the IAT is at a relatively low amplitude (condition 1 in Fig. 1). As the IAT grows due to drifting electrons so does the wave-driven Ohmic heating of the electrons. This raises the temperature of the plasma, leading to enhanced ionization (condition 2). The high plasma density slows the electrons by continuity and therefore reduces the growth of the IAT (condition 3). This, in turn, reduces wave-driven heating and cools the plasma. As a result, ionization drops and the electron velocity rises again (condition 4). Physically, we might expect that the onset criterion for such an instability should be due to greater growth in the IAT, while ionization acts as a restoring process. Ultimately, this would be ascribed to a wave-particle interaction between the IAT and the background plasma and could be classified as a wave-driven ionization instability.

Thinking about this process more quantitatively, step 1 in Fig. 1 can be captured by the electron energy equation and ion continuity equation, where as step 2 is due to electron continuity. Step 3 is a result of the wave-kinetic equation (Eqn. 3) and electron energy. Step 4 again relies on the continuity of ions and electrons. In sum, we need four equations to describe this process in a reduced zero-dimensional model. Ion continuity is given by

$$\frac{\partial n}{\partial t} + \nabla \cdot (n u_i) = n \nu_{ion} \ , \tag{5}$$

where n is the plasma density, ν_{ion} is the ionization rate and $\nu_{ion,0}$ is the steady state ionization rate. Electron continuity is

$$\frac{\partial n}{\partial t} + \nabla \cdot (n u_e) = n \nu_{ion} \Rightarrow \nabla \cdot (n u_e) = \nabla \cdot (n u_i), \tag{6}$$

where u_e is the electron drift velocity. Since $u_i \ll u_e$ we simplify the electron continuity to

$$\nabla \cdot (n u_e) \simeq 0 \Rightarrow n u_e = \frac{I}{qA} \ . \tag{7}$$

In this case, we will further assume that there are steady state density, velocity and wave energy gradients, while neglecting those in temperature[15]. Given our assumptions, the electron energy equation can be simplified to

$$\frac{3}{2}\frac{\partial nT_e}{\partial t} - u_e \nabla \cdot (nT_e) = n m_e u_e^2 \nu_{an}(W, n, T_e) \ , \tag{8}$$

where T_e is the electron temperature, m_e is the electron mass, and ν_{an} is the total wave-driven collision frequency that is well known to dominate the plasma. Lastly, by summing Eqn. 3 over modes we arrive at the total wave energy density conservation equation for the IAT

$$\frac{\partial W}{\partial t} + \nabla \cdot (v_g W) = W \omega_0 \frac{u_e}{v_e} \ , \tag{9}$$

where W now denotes the total wave energy density in the turbulence, ω_0 is the average frequency of the IAT spectrum, and v_e is the thermal velocity of electrons, and $v_g = c_s + u_i$ is the IAT group velocity. Note that for simplicity we have neglected the damping terms. Eqns. 5 - 9 consist of a complete set of equations that we can solve through a linear perturbation analysis.

We conduct a linear perturbation of this system of equations of the form $n = n_0 + n_1 e^{-i\omega t}$. Furthermore, for simplicity we solve this problem in the frame of the ions such that $u_{i0} = 0$ but $\nabla(u_{i0}) \neq 0$. First examining the steady state conditions,

$$\nabla(n_0) + n_0 \nabla \cdot u_{i0} = n_0 \nu_{ion,0} \Rightarrow \nabla \cdot u_{i0} = \nu_{ion} \tag{10}$$

$$n_0 u_{e0} = \frac{I_0}{qA} \tag{11}$$

$$-T_{e0} \nabla(n_0) = n_0 m_e u_{e0} \nu_{an,0} \tag{12}$$

$$v_g \nabla \cdot (W_0) = W_0 \omega_0 M_{e0} \ . \tag{13}$$

Using these steady state expressions, we can perturb and linearize the equations to find

$$\frac{-i\omega}{\gamma_{ion}}\frac{n_1}{n_0} = \frac{T_{e1}}{T_{e0}} \ , \ \gamma_{ion} \equiv T_{e0} \frac{\partial \nu_{ion}}{\partial T_e}\Big|_{T_e = T_{e0}} \tag{14}$$

$$\frac{n_1}{n_0} = -\frac{u_{e1}}{u_{e0}} \tag{15}$$

$$2\frac{T_{e1}}{T_{e0}} = \frac{u_{e1}}{u_{e0}} + \frac{W_1}{W_0} + \frac{1}{2}\frac{n_1}{n_0} \tag{16}$$

$$-\left(\frac{i\omega}{\gamma_{IAT}} + 1\right)\frac{W_1}{W_0} = \frac{u_{e1}}{u_{e0}} - \frac{T_{e1}}{T_{e0}} \ , \ \gamma_{IAT} \equiv v_g \frac{\nabla \cdot W_0}{W_0} \ . \tag{17}$$

Here we have made the additional assumption, based on experimental measurements, that $\omega \ll \nu_{an}$, and that current fluctuations are small compared to the density and velocity. The parameter, γ_{ion}, is the response of ionization to changes in temperature while γ_{IAT} is the temporal growth rate of the IAT. Physically, Eqn. 5 says that the plasma density lags the fluctuations in electron temperature, while Eqn. 7 shows that a rise in density corresponds to reduced a electron drift. The temperature will depend on the wave energy of the turbulence, density, and velocity. The IAT wave energy responds to changes in velocity and temperature. Solving this system of equations, it can be shown that the real and imaginary components of the frequency are

$$\omega_r = \sqrt{\frac{\gamma_{IAT}\gamma_{ion}}{2}} \tag{18}$$

$$\omega_i = \gamma_{ion}\left(\frac{2\gamma_{IAT}}{\gamma_{ion}} - 1\right) \ . \tag{19}$$

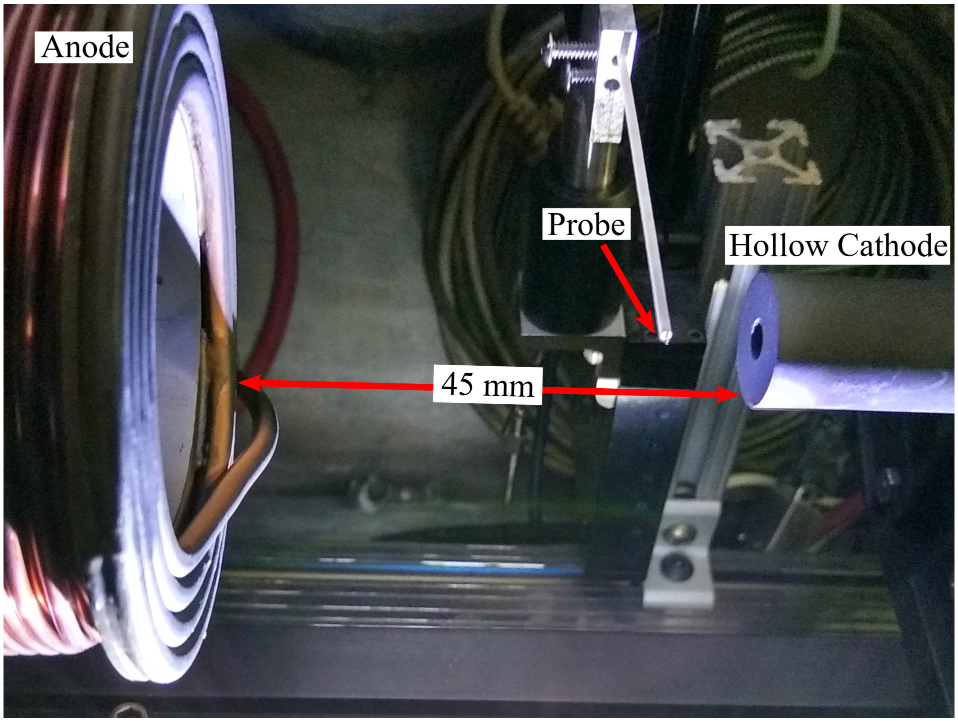

Fig. 2 Experimental setup.

We find that the real frequency is the geometric mean of the IAT growth rate and the ionization response rate. The onset criterion given by the imaginary component indicates that if the IAT grows faster than the plasma can respond to ionization then in the instability will grow. Physically, this result indicates that the mode is driven unstable when the IAT heats the plasma faster than it can cool itself by ionization. This analytical result follows the physical picture we previously described in Fig. 1.

IV. Experimental Methods

For this investigation, we used a LaB_6 hollow cathode that was operated on xenon at 20 A of discharge current at and flow rates between 8 and 4 sccm which and a discharge voltages between 21 and 35 V. The anode was 45 mm downstream of the keeper exit. The discharge was established in a 0.5 m $\times$ 1 m vacuum chamber that is cryogenically pumped and achieves a base pressure of 0.12 μTorr. At our selected operating conditions, the operating pressure is between 10-30 μTorr-Xe. With our electrostatic diagnostics, we measure the ion saturation current, floating potential, and plasma potential as a function of position on the time-scale of the ionization oscillation. The time-resolved waveforms of these parameters are captured at 10 MHz using an oscilloscope. Fig. 2 shows the experimental setup. The emissive probe (measures plasma potential) is mounted below the Langmuir probe (measures saturation current and floating voltage). A vertical motion stage allows us to make measurements of plasma oscillations for all probes on the discharge axis. An axial motion stage is used to translate the cathode and anode to sample the plume along the discharge axis with a 1 mm resolution.

V. Experimental Results

Here we present our experimental results. We have divided this section into three parts. First, assess the validity of our physical picture by plotting the critical plasma parameters identified by our theory. We further investigate the bounds of validity of the reduced-order model by comparing with different levels of instability. Next, we examine our onset criterion and real frequency in the plume to determine if the theory describes the observed trends.

A. Validation of the Physical Picture

To validate the physical picture from Fig. 1, we need to calculate the density, temperature, electron drift velocity, and the IAT wave energy as a function of time. To calculate these plasma parameters, we follow the technique use in [16]. In brief we use the emissive, floating, and ion saturation probes to determine electric field, temperature, and density. These parameters are used to infer the electron drift velocity from the electron continuity equation using ionization as a source term and assuming a conical expansion of the plasma from the keeper orifice to the anode. Time resolution is achieved by using the discharge current as a reference and a phase averaging to determine how these parameters evolve as a function of phase angle, θ with respect to the discharge current oscillation. The equations necessary for this calculation are

$$E = -\nabla\Phi \ , \ T_e = \frac{2(\Phi - V_f)}{\ln\left(\frac{2}{\pi}\frac{m_i}{m_e}\right)} \text{ , and } n = \frac{I_{sat}}{0.61 A_p c_s}, \tag{20}$$

where E is the electric field, Φ is the plasma potential, V_f is the floating voltage, I_{sat} is the ion saturation current and A_p is the probe surface area. These quantities can be used to evaluate the electron continuity equation to estimate the electron drift velocity

$$u_e(z,t) = \frac{\int_{z_0}^{z}\left(n(z,t)\nu_{ion}(z,t) - \frac{\partial n(z,t)}{\partial t}\right)A(z)dz}{n(z,t)A(z)} + \frac{n(0,t)}{n(z,t)}\frac{A(0)}{A(z)}u_e(0,t) \ , \tag{21}$$

where ν_{ion} is the ionization rate calculated from Ref. 20 and $A(z)$ is the cross-sectional area of the plasma. The boundary condition for velocity is $u_e(0,t) = I_{dc}(t)/qn(0,t)A(0)$ and is applied to our closest measurement to the cathode. We estimate the wave energy by calculating the Fourier transform of the ion saturation current signal over a short time constant ($\tau = 1.75$ μs) and using Eqn. 3, summing of the IAT contributions of the spectrum (see Fig. 3). This technique has been used to analyze fluctuations in turbulence level in Refs. [15,16,21].

Before examining the time-evolution of the plasma parameters, we first show in Fig. 3 the Fourier spectrum measured by the probes at each of our three operating conditions. At the higher flow rate (8 sccm) in Fig. 3a, we see the first harmonic of the ionization instability at 57 kHz in both the ion saturation probe and the discharge current. This single peak indicates that the ionization instability is sinusoidal in nature under these conditions. In the probe signal, we also find higher frequency modes that are associated with IAT. At 6 sccm, (Fig. 3b), we see the fundamental oscillation frequency of 57 kHz for the ionization instability, but also higher harmonics that indicate non-sinusoidal behavior. The amplitude of these oscillations has also increased relative to the background discharge and ion saturation currents. At the lowest flow rate, shown in Fig. 3c we see further evidence of the non-sinusoidal perturbation of the plasma by the ionization instability as well as the presence of the IAT. In sum, Figs. 3a - 3c indicate that at lower flow rates the instability is stronger and is able to excite higher harmonics, which is indicative of non-linear behavior.

Now that we have established the spectral characteristics of the plasma, in Fig. 4 we show the resulting relative fluctuations of the time-resolved analysis at a single location in the plume ($z =$

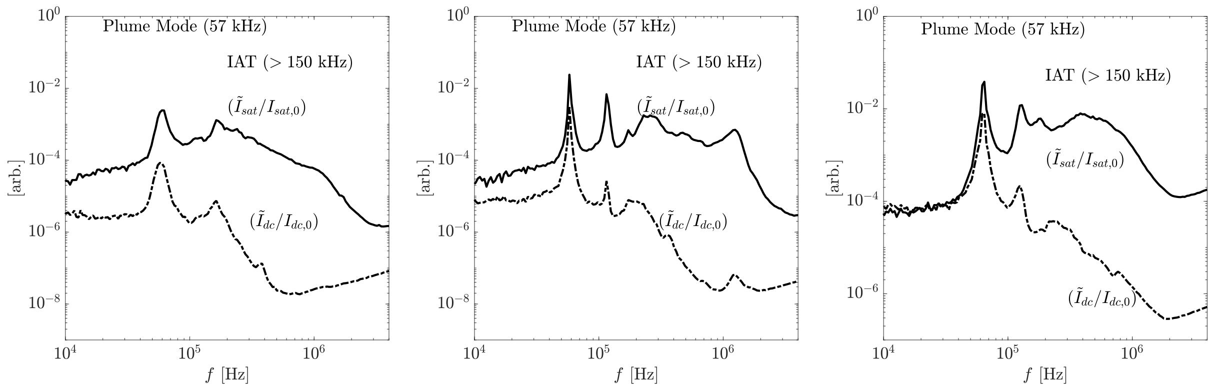

(a) $\dot{m} = 8$ **sccm.** **(b)** $\dot{m} = 6$ **sccm.** **(c)** $\dot{m} = 4$ **sccm.**

Fig. 3 Fourier spectrum of the ion saturation current and the discharge current at three operating conditions.

14 mm). At high-flow rates (Fig. 4a), we see that the amplitude of the current is density is very low $\mathcal{O}(10^{-3})$ where as the density, temperature and velocity are one order of magnitude larger and the wave energy is two orders. In this figure, we see that the wave energy leads the temperature in phase and that the density lags the temperature. This is consistent with an ionization-type instability. Furthermore, the we find that the density and the velocity are out of phase, which is consistent with the fact that current is almost conserved. Overall, the results in Fig. 4a are consistent with the physical picture we have proposed for this turbulence-driven ionization instability.

Figure 4b shows these same parameters at a lower flow rate, $\dot{m} = 6$ sccm. At this condition, the relative fluctuations in all the plasma parameters have increased and we can see the beginnings of non-linear behavior in the instability. In Fig. 4a, we see approximately sinusoidal oscillations, whereas now in Fig. 4b we find peaked structures in temperature, density, and velocity that were not previously apparent. Although the current fluctuations are two orders of magnitude larger at this lower flow rate, the density and velocity oscillations are still out of phase, providing the necessary feedback on the turbulent energy to sustain the instability.

Figure 4c, again, shows the evolution of these critical plasma parameters as a function of time, but at the 4 sccm test point. At this extremely low flow rate, the peak-to-peak fluctuations in current density are $\mathcal{O}(0.5)$, meaning they are on the same order as the steady discharge current. At this condition the fluctuations in wave energy exceed the mean value and there is evidence of higher harmonics as indicated by the power spectrum in Fig. 3c. The density, and temperature are highly peaked and in fact, the density appears to lead the temperature in phase. Furthermore, the electron drift velocity is no longer completely out of phase with the density. This finding is consistent with the fact that we observed significant fluctuations in current that destroy this relationship. In sum, at such extreme cases, where the instability is very large, the behavior is non-linear and not properly captured by our theory.

In sum, the results from Figs. 4a - 4c indicate that when the current oscillations are relatively low level, the physical picture supported by the theory is able to qualitatively describe the process we observe. As the flow rate decreased, we find evidence of non-linear behavior that in some cases, notably in Fig. 4c, our physical picture does not hold and we therefore cannot expect that the linear theory will properly describe these conditions. For a more quantitative analysis, in the following section we use these measurements to examine the predicted instability criterion and real frequency for the 8 sccm flow rate.

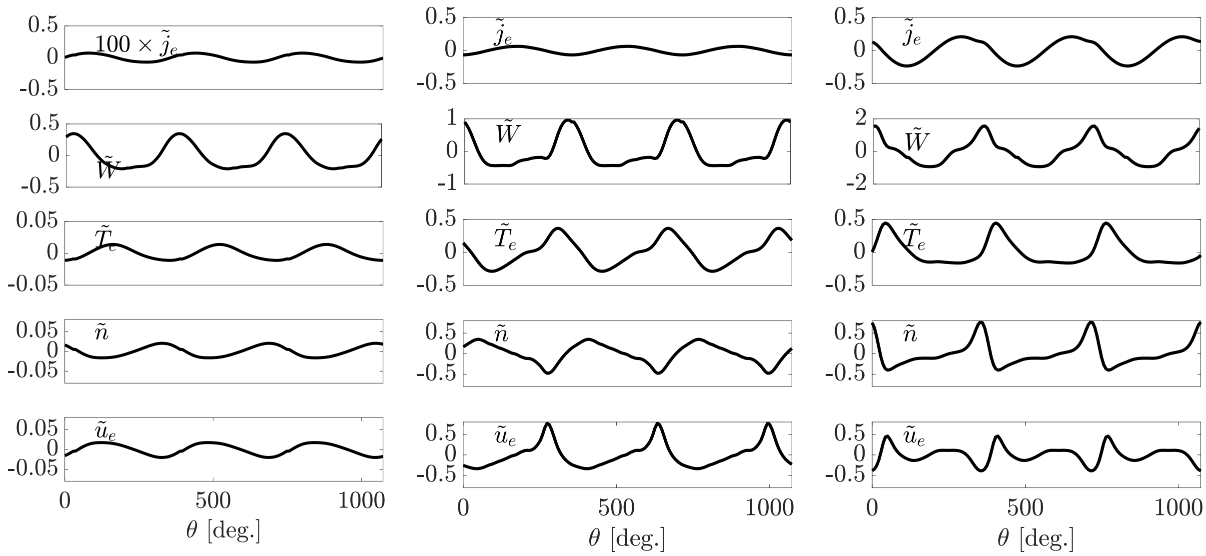

(a) $\dot{m} = 8$ **sccm.**

(b) $\dot{m} = 6$ **sccm.**

(c) $\dot{m} = 4$ **sccm.**

Fig. 4 Relative fluctuations in current density, IAT wave energy density, electron temperature, density, and electron drift velocity at $z = 14$ mm from the cathode.

B. Evaluation of Stability Criterion for the Turbulence-driven Ionization Instability

In Sec. A, we have determined that our linear theory would likely on properly capture the dynamics of our highest flow rate condition since non-linear behavior appears to become important at the other lower flow rate points. There, we show in Fig. 5 a plot of the real and imaginary growth rates. To determine γ_{IAT}, we have measured the wave energy in the turbulent modes and evaluated Eqn. 17 with an estimated the ion drift velocity of 3 km/s. We evaluate γ_{ion} using our estimate of neutral density and our measurement of temperature in the plume. Our theory is presented in the frame of the ions, where as our measurements are made in the laboratory frame where the ions are drifting. As a result, the waves will appear to grow spatially, when Doppler shifted by the ion drift. For example for the plasma potential

$$\tilde{\Phi} = \Phi_1 e^{-i(\omega + i\omega_i)t} \ , \ x_0 = x - u_{i0}t \ \Rightarrow \tilde{\Phi} = \Phi_1 e^{-i(\omega+i\omega)\frac{x-x_0}{u_{i0}}} \equiv \Phi_1 e^{-i(k+ik_i)(x-x_0)} \tag{22}$$

As a result, we can expect a temporal growth of the waves, ω_i, to appear as steady-state spatial growth, $k_i \equiv \omega_i/u_i$. With this in mind, we find that, near the cathode, the growth rate of the turbulence-driven ionization instability is large and continues to grow till $z = 21$ mm downstream of the cathode. At this position, the real frequency peaks at around 35 kHz, within a factor of two from our fundamental frequency of 57 kHz. Beyond this point, we predict that the mode is damped. Additionally, we also show in Fig. 5 the peak-to-peak plasma potential fluctuations where we find that these oscillations increase in amplitude near the cathode and are damped downstream as predicted by the theory and the Doppler shifted growth in Eqn. 22.

VI. Discussion

Having examined, in detail, the physical picture and onset criterion for this turbulence-driven, ionization instability we now turn our attention to the implications of our first-principles, analytical theory for hollow cathodes. Although we have established a specific onset criterion, it is perhaps more convenient to recast this into cathode operating parameters like mass flow rate and discharge

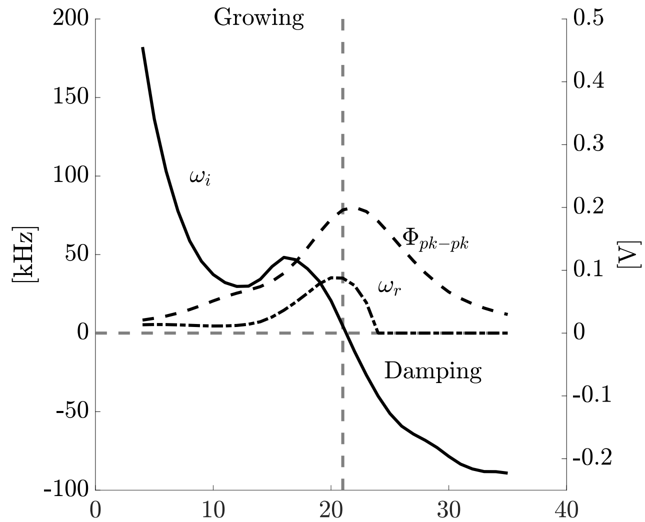

Fig. 5 Real and imaginary frequency calculated from Eqn. 19 and peak-to-peak plasma potential fluctuations. $\dot{m} = 8$ sccm.

current. Given the dependence on the growth rate of the turbulence on the electron drift, we can say that

$$\gamma_{IAT} = \omega_0 \frac{u_e}{v_e} = \omega_0 \frac{nqu_eA_o}{nqv_eA_o} = \omega_0 \frac{I_{dc}}{I_{th}} \ , \tag{23}$$

where A_o is the orifice cross sectional area and ω_0 is the average frequency of the IAT spectrum and I_{th} is the thermal electron current. The response of ionization can be shown to

$$\gamma_{ion} = T_{e0} \frac{\partial \nu_{ion}}{\partial T_e} \simeq \nu_{ion} = \frac{n\nu_{ion}}{n} = \frac{\nabla(n_n u_n)}{n} \sim \frac{\dot{m}}{nm_iA_oL} \ \text{ or } \ \frac{1}{\alpha}\nu_n, \tag{24}$$

where n_n is the neutral density, $\dot{m}$ is the propellant mass flow rate, L is the neutral gradient length scale, $\alpha = n/n_n$ is the ionization fraction (in the weakly ionized limit) and ν_n is the neutral transit frequency. Combining these, we can modify our onset criterion to be

$$2\frac{I_{dc}A_oL}{\dot{m}} > \frac{I_{th}}{\omega_0 n m_i} \ \text{ or } \ 2\alpha\frac{I_{dc}}{I_{th}} > \frac{\nu_n}{\omega_0} \ . \tag{25}$$

The first is the well known empirical scaling law for the cathode plume mode[4], onset is achieved by either increasing the current reducing the flow rate. In addition, our result suggests that the ionization instability can typically be suppressed by reducing the orifice size. Furthermore, it has been noted experimentally that increasing the cathode-to-anode gap can cause the onset of this ionization instability. If we take the neutral gradient length scale to be proportional to this distance, then the criterion we have derived is again in agreement with empirical scaling laws.[22] Alternatively, in Eqn. 25 we have an alternative criterion that indicates that if the directed current is greater than the thermal current and the ionization fraction is large, then the instability will onset. This is in keeping with our physical picture of an ionization wave (where the ionization fraction is a critical parameter) that is driven unstable by the turbulence that is present in the plasma as a result of the large current drawn from the cathode.

VII. Conclusions

In conclusion, we have for the first time derived a stability criterion for the onset of the ionization instability associated with the cathode plume mode and arrived at an intuitive physical mechanism, in the small oscillation limit, by which the plasma oscillates between a cold and hot state. The mode is driven unstable when wave-driven heating of the plasma exceeds cooling through ionization. Experimental measurements of this instability show that the conditions for instability are met near the cathode but not downstream near the anode. The observed local maximum in plasma potential fluctuations is indicative of a localized region from which the instability propagates. By examining the time-evolution of key plasma parameters, we have shown that qualitatively the time-variation of these quantities is in keeping with the physical picture and the linearized equations. Lastly we have recast the derived onset criterion and found that it reduces to the empirically derived criterion, but also predicts a strong dependence on electron temperature that could be harnessed to improve future cathode designs.

Acknowledgements

This work was funded by the NASA Space Technology Research Fellowship under grant number NNX15AQ37H.

References

[1] I. Mikellides, Ira Katz, and Dan Goebel. Model of the Plasma Potential Distribution in the Plume of a Hollow Cathode. In *40th AIAA/ASME/SAE/ASEE Joint Propulsion Conference and Exhibit*, Fort Lauderdale, Florida, July 2004. American Institute of Aeronautics and Astronautics. ISBN 978-1-62410-037-6. doi: 10.2514/6.2004-4108. URL `http://arc.aiaa.org/doi/10.2514/6.2004-4108`.

[2] Ioannis G. Mikellides, Ira Katz, Dan M. Goebel, and Kristina K. Jameson. Evidence of nonclassical plasma transport in hollow cathodes for electric propulsion. *Journal of Applied Physics*, 101(6):063301, March 2007. ISSN 0021-8979. doi: 10.1063/1.2710763. URL `http://aip.scitation.org/doi/abs/10.1063/1.2710763`.

[3] George A. Csiky. Measurements of some properties of a discharge from a hollow cathode. *NASA Technical Note*, 1969. URL `https://ntrs.nasa.gov/archive/nasa/casi.ntrs.nasa.gov/19690008515.pdf`.

[4] Verlin J. Friedly and Paul J. Wilbur. High current hollow cathode phenomena. *Journal of Propulsion and Power*, 8(3):635–643, 1992. ISSN 0748-4658. doi: 10.2514/3.23526. URL `http://dx.doi.org/10.2514/3.23526`.

[5] M. Mandell and I. Katz. Theory of hollow operation in spot and plume modes. American Institute of Aeronautics and Astronautics, June 1994. doi: 10.2514/6.1994-3134. URL `http://arc.aiaa.org/doi/10.2514/6.1994-3134`.

[6] Ioannis G. Mikellides, Ira Katz, Dan M. Goebel, Kristina K. Jameson, and James E. Polk. Wear mechanisms in electron sources for ion propulsion, II: Discharge hollow cathode. *Journal of Propulsion and Power*, 24(4):866–879, 2008. URL `http://arc.aiaa.org/doi/pdf/10.2514/1.33462`.

[7] R. Z. Sagdeev and A. A. Galeev. *Nonlinear Plasma Theory*. 1969. URL `http://adsabs.harvard.edu/abs/1969npt..book.....S`.

[8] R. C. Davidson and N. A. Krall. Anomalous transport in high-temperature plasmas with applications to solenoidal fusion systems. *Nuclear Fusion*, 17(6):1313, 1977. ISSN 0029-5515. doi: 10.1088/0029-5515/17/6/017. URL `http://stacks.iop.org/0029-5515/17/i=6/a=017`.

[9] V. Yu. Bychenkov, V. P. Silin, and S. A. Uryupin. Ion-acoustic turbulence and anomalous transport. *Physics Reports*, 164(3):119–215, July 1988. ISSN 0370-1573. doi: 10.1016/0370-1573(90)90122-I. URL `http://www.sciencedirect.com/science/article/pii/037015739090122I`.

[10] Benjamin A. Jorns, Ioannis G. Mikellides, and Dan M. Goebel. Ion acoustic turbulence in a 100-A LaB6 hollow cathode. *Physical Review E*, 90(6):063106, December 2014. doi: 10.1103/PhysRevE.90.063106. URL `http://link.aps.org/doi/10.1103/PhysRevE.90.063106`.

[11] Benjamin A. Jorns, Christoper Dodson, Dan M. Goebel, and Richard Wirz. Propagation of ion acoustic wave energy in the plume of a high-current LaB6 hollow cathode. *Physical Review E*, 96(2):023208, August 2017. doi: 10.1103/PhysRevE.96.023208. URL https://link.aps.org/doi/10.1103/PhysRevE.96.023208.

[12] Gaétan Sary, Laurent Garrigues, and Jean-Pierre Boeuf. Hollow cathode modeling: I. A coupled plasma thermal two-dimensional model. *Plasma Sources Science and Technology*, 26(5):055007, 2017. ISSN 0963-0252. doi: 10.1088/1361-6595/aa6217. URL http://stacks.iop.org/0963-0252/26/i=5/a=055007.

[13] Alejandro Lopez Ortega, Benjamin A. Jorns, and Ioannis G. Mikellides. Hollow Cathode Simulations with a First-Principles Model of Ion-Acoustic Anomalous Resistivity. *Journal of Propulsion and Power*, 34(4): 1026–1038, 2018. ISSN 0748-4658. doi: 10.2514/1.B36782. URL https://doi.org/10.2514/1.B36782.

[14] Dan M. Goebel, Kristina K. Jameson, Ira Katz, and Ioannis G. Mikellides. Potential fluctuations and energetic ion production in hollow cathode discharges. *Physics of Plasmas (1994-present)*, 14(10):103508, October 2007. ISSN 1070-664X, 1089-7674. doi: 10.1063/1.2784460. URL http://scitation.aip.org/content/aip/journal/pop/14/10/10.1063/1.2784460.

[15] Marcel P. Georgin, Benjamin A. Jorns, and Alec D. Gallimore. Correlation of ion acoustic turbulence with self-organization in a low-temperature plasma. *Physics of Plasmas*, 26(8):082308, August 2019. ISSN 1070-664X. doi: 10.1063/1.5111552. URL https://aip.scitation.org/doi/full/10.1063/1.5111552.

[16] Marcel P. Georgin, Benjamin Jorns, and Alec Gallimore. Time-varying Non-classical Collisions and Turbulence in a Hollow Cathode. In *AIAA Propulsion and Energy 2019 Forum*, Indianapolis, IN, August 2019. American Institute of Aeronautics and Astronautics. ISBN 978-1-62410-590-6. doi: 10.2514/6.2019-4079. URL https://arc.aiaa.org/doi/10.2514/6.2019-4079.

[17] Ioannis G. Mikellides, Pablo Guerrero, Alejandro Lopez Ortega, and James E. Polk. Spot-to-plume Mode Transition Investigations in the HERMeS Hollow Cathode Discharge Using Coupled 2-D Axisymmetric Plasma-Thermal Simulations. American Institute of Aeronautics and Astronautics, July 2018. ISBN 978-1-62410-570-8. doi: 10.2514/6.2018-4722. URL https://arc.aiaa.org/doi/10.2514/6.2018-4722.

[18] Gaétan Sary, Laurent Garrigues, and Jean-Pierre Boeuf. Hollow cathode modeling: II. Physical analysis and parametric study. *Plasma Sources Science and Technology*, 26(5):055008, 2017. ISSN 0963-0252. doi: 10.1088/1361-6595/aa6210. URL http://stacks.iop.org/0963-0252/26/i=5/a=055008.

[19] Benjamin Jorns, Alejandro Lopez Ortega, and Ioannis G. Mikellides. First-principles Modelling of the IAT-driven Anomalous Resistivity in Hollow Cathode Discharges I: Theory. American Institute of Aeronautics and Astronautics, July 2016. ISBN 978-1-62410-406-0. doi: 10.2514/6.2016-4626. URL http://arc.aiaa.org/doi/10.2514/6.2016-4626.

[20] Dan M. Goebel and Ira Katz. *Fundamentals of electric propulsion: ion and Hall thrusters*, volume 1. John Wiley & Sons, 2008. URL http://books.google.com/books?hl=en&lr=&id=P5OGFXcBKcwC&oi=fnd&pg=PR5&dq=%22Electrode+Breakdown%22+%226:+Hollow%22+%22Ionization+Length+and+Scaling%22+%22Dielectric-Wall+Versus+Metallic-Wall+Comparison%22+%22Dispenser+Cathodes+in+Insert%22+%22Hall+Thruster%22+%22Pyrolytic+Graphite%22+%22Hollow+Cathode+Operation%22+%22TAL+Hall+Thruster+Efficiency+(Metallic+Walls&ots=Sbv2zvFn6h&sig=jItSQOscncTmqCz26jx_rAYmlbc.

[21] Sedina Tsikata and Tiberiu Minea. Modulated Electron Cyclotron Drift Instability in a High-Power Pulsed Magnetron Discharge. *Physical Review Letters*, 114(18):185001, May 2015. doi: 10.1103/PhysRevLett.114.185001. URL https://link.aps.org/doi/10.1103/PhysRevLett.114.185001.

[22] George-Cristian Potrivitu, Romain Joussot, and Stéphane Mazouffre. Anode position influence on discharge modes of a LaB6 cathode in diode configuration. *Vacuum*, 151:122–132, May 2018. ISSN 0042-207X. doi: 10.1016/j.vacuum.2018.02.010. URL http://www.sciencedirect.com/science/article/pii/S0042207X17314343.